Available online at www.sciencedirect.com
SCIENCE DIRECT®
Journal of Sound and Vibration 293 (2006) 485–495
JOURNAL OF SOUND AND VIBRATION
www.elsevier.com/locate/jsvi

The use of decay rates to analyse the performance of railway track in rolling noise generation

C.J.C. Jones[a,*], D.J. Thompson[a], R.J. Diehl[b]

[a]Institute of Sound and Vibration Research, University of Southampton, Southampton, UK
[b]Müller BBM GmbH, Munich, Germany

Accepted 26 August 2006
Available online 7 February 2006

Abstract

Through the development and testing of theoretical models for rolling noise in the past, it has been well demonstrated that the rate of decay of vibration along the rail is closely linked to the noise performance of the track, since it controls the effective radiating length of the rail. The decay rates of vibration along the rail have long been used by researchers as an intermediate, measurable parameter by which to test and improve the accuracy of prediction models. Recently, it has been suggested that the decay rates should be used as a criterion for the selection of track for noise measurements that are part of the acceptance testing of interoperable trains in Europe. In this context, a more detailed understanding of the factors that affect the measurement of decay rates and a consistent approach to the data processing have become important topics. Here, a method is suggested for the calculation of decay rates from frequency response measurements. Different effects are shown in the measured decay rates of a ballasted track with mono-bloc sleepers, a slab track and a ballasted track with bi-bloc sleepers. In the last case, a model for a periodically supported track is used to study the effects observed. It is shown that a peak in the decay rate just above the pinned–pinned frequency may be overestimated because of the measurement procedure that has been used.

1. Introduction

The regulations governing the use of rolling stock internationally in Europe (on the Trans European Network) are embodied in the Technical Specifications for Interoperability (TSI's) for conventional- [1], and high-speed trains [2]. These set out the acceptance tests for vehicle types and include tests of their noise performance. In order to ensure a fair assessment of rolling stock in different countries, the track on which pass-by noise is measured is to be controlled, at least to the extent that it must be a relatively quiet track. By this means it should have as low an influence as possible on the measured noise level. Even if it is still an important contributor to the rolling noise, by controlling the track's acoustic performance, its contribution should be consistent. Currently, the acoustic parts of both TSI's are being improved and, as part of this, it has been suggested that the track's acoustic performance (in terms of sound generated per unit roughness) be

*Corresponding author. Tel.: +44 2380 593224; fax: +44 2380 593190.
E-mail addresses: cjcj@isvr.soton.ac.uk (C.J.C. Jones), rolf.diehl@mbbm.de (R.J. Diehl).

0022-460X/$ - see front matter
doi:10.1016/j.jsv.2005.08.060

characterised by measurements of its decay rates. These proposals are being tested in an international programme of measurements known as the Noemie project. The issues surrounding the TSI's and the Noemie project are covered in Ref. [3]. Here, some technical issues are investigated regarding the measurement and calculation of decay rates.

The decay rates of vibration with distance along the rail have for many years been measured for the purpose of informing and validating models for rolling noise [4–6] and measurements have already become more or less routine to the noise experts of some railways. The Noemie project has offered the opportunity for experience of decay rate measurement to become more widespread in anticipation of its adoption in the TSI's. This process has itself highlighted the need for a consistent and robust approach to calculating decay rates from measurement data in order to reduce the variation in results. It has also given rise to a need for a discussion of decay rate measurements and the relationship of such data to the models. This has been the motivation for the present paper.

2. Decay rates as an indicator of the acoustic performance of the track

The mechanisms leading to the generation of rolling noise from railway vehicles on plain track are well known and have been demonstrated through the development and validation of theoretical models such as TWINS [4,7,8]. As a wheel rolls along a rail, the roughnesses of the two rolling surfaces add together to excite vibration in each component by imposing a time-varying relative displacement across the contact. The roughness excites frequencies of vibration depending on the speed of the vehicle v according to $f = v/\lambda$ where λ is the wavelength. The combined roughness of the wheel and rail is broadband in character and the wavelength range of interest is from a few millimetres, where the amplitudes are typically less than a micron, to about 0.5 m, at which the amplitude reaches the order of 100 μm. These wavelengths correspond approximately, for conventional train speeds, to the frequency range from about 50 Hz to 5 kHz. At higher frequencies the small wavelengths of roughness involved are averaged out over the length of the wheel–rail contact patch.

The imposed relative displacement is taken up as vibration of the wheel, the rail or the deformation in the contact, the response of each being determined by their relative point receptances [9]. At frequencies above about 1.5 kHz, the wheel exhibits resonance frequencies at which the radial receptance exceeds that of either the rail or the contact spring. In this frequency range therefore, the wheel is strongly excited into vibration and is, generally, a greater source of noise than the rail. At frequencies lower than this, the point receptance of the rail is the highest of the three and it is therefore the track that responds to the roughness excitation and becomes the dominant noise source. Below about 400 Hz (depending on the pad stiffness), the sleeper is responsible for most of the track component of noise, and above this frequency the rail is more important. In many cases, especially for conventional speeds, the rail is the greatest radiator of rolling noise overall.

The sound power, W, radiated by the rail can be estimated from the vibration of the track using the general formula for predicting acoustic radiation

$$W = A\sigma\rho_0 c_0 \langle v^2 \rangle, \tag{1}$$

where A is the surface area of the radiator, $\langle v^2 \rangle$ is the spatially averaged mean square surface-normal velocity of vibration in the frequency band, σ is the radiation ratio of the radiator and $\rho_0 c_0$ is the specific acoustic impedance of air. The rail can be regarded as an infinitely long radiator with vibration waves of different types propagating along it (e.g. vertical or lateral rigid cross-sectional motion, or the cross-sectional mode shape of a higher order wave; both near field and propagating waves). In the theoretical models [7], the sound power calculation is split into components arising from each wave type. The velocity of the rail surface can then be expressed as a wave-type cross-sectional motion and the rate of decay of the vibration amplitude with distance from wheel–rail contact at which the response to the roughness is calculated.

A simple track model, used in the validation of TWINS [4,7,8], describes the rail as a Timoshenko beam on a two-layer continuous support representing the rail pad and ballast stiffness with a layer of mass between representing the sleepers [10]. Equivalent models are used separately for the vertical and lateral bending waves of the rail. The effects of a dynamic stiffness of the ballast layer and modal behaviour of the sleepers may also be included. This model has been shown to produce good predictions of rail noise [4,8], even though it does not account for the cross-sectional mode wave motion that occurs in the rail above about 1.5 kHz nor the effects of the discrete supports.

If the velocity field of the rail section is assumed to consist of rigid vertical or lateral motion, of amplitude v_{wave}, in correspondence with the vertical and lateral bending waves included in the simple track model, the sound power for a single wave of vertical or lateral motion can be expressed as

$$W_{\text{wave}} = \widetilde{W}_{\text{wave}} \int_{-\infty}^{\infty} |v_{\text{wave}}(z)|^2 \, \mathrm{d}z, \tag{2}$$

where $\widetilde{W}_{\text{wave}}$ is the sound power per unit length radiated from a vertical or lateral unit velocity motion. $\widetilde{W}_{\text{wave}}$ is evaluated by assuming a two-dimensional acoustic field since, generally, the bending wavelengths in the rail are longer than those in air (a correction can be carried out for some three-dimensional behaviour below 250 Hz [11]). $v_{\text{wave}}(z)$ represents the variation of the vertical or lateral bending wave motion along the rail.

Vertical and lateral waves in the rail (both the near field and propagating waves) are assumed to decay exponentially with distance z from the excitation point (wheel contact) so that $|v_{\text{wave}}(z)| = v_{\text{wave}}(0)\mathrm{e}^{-\beta_{\text{wave}}|z|}$ where β_{wave} is the decay constant specific to that wave. The sound power from the vertical or lateral waves in the rail can be estimated therefore as

$$W_{\text{wave}} = \widetilde{W}_{\text{wave}} \int_{-\infty}^{\infty} v_{\text{wave}}^2(0)\mathrm{e}^{-2\beta_{\text{wave}}|z|} \, \mathrm{d}z = 2\widetilde{W}_{\text{wave}} v_{\text{wave}}^2(0) \int_{0}^{\infty} \mathrm{e}^{-2\beta_{\text{wave}}|z|} \, \mathrm{d}z = 2\widetilde{W}_{\text{wave}} v_{\text{wave}}^2(0) \frac{1}{2\beta_{\text{wave}}} \tag{3}$$

β_{wave} can be converted to a decay rate expressed in dB per metre, Δ, as

$$\Delta = 20 \log_{10}(\mathrm{e}^{\beta_{\text{wave}}}) = 8.686\beta_{\text{wave}} \, \mathrm{dB/m}. \tag{4}$$

Eq. (3) shows that the vertical and lateral decay rates are direct factors in the determination of rail noise. In fact, since the sleepers are excited from the rail also, they are similarly related to the sleeper component of noise.

3. Measurement and calculation of decay rates

The decay rates must be calculated from a set of transfer response measurements to different distances along the rail. Since this is the case, without performing an experimental wavenumber decomposition [6] that would be impractical for the purposes of the TSI's, the decay rates must be based upon the total response from all waves excited either vertically or laterally rather than for individual wave types. Thus the decay rates that are measured are *effective overall* vertical or lateral decay rates and encompass the behaviour of all waves, near field and propagating. These, nevertheless, are a more direct measure of the acoustic performance of a track than those of an individual wave. Although the acoustic performance also depends on the radiation efficiency of the rail, etc., such decay rates are a suitable measure given that, practically, the rail section does not change much for conventional railway and high-speed tracks in Europe and that neither does the situation that the rail receptance exceeds the wheel receptance for the frequency range below wheel web-bending resonances.

To obtain the necessary transfer response data, a measured force impulse is applied on the rail head with an instrumented hammer. Rather than move the accelerometer to each measurement distance in turn, it is more convenient to move the hammer position. Measurements are made of the vertical response to vertical excitation and lateral response to lateral excitation. There is no need to measure the cross-transfer functions. Either the accelerance or, if analogue integration is available, mobility can be measured. The latter has been found to produce better quality data at low frequency because of the dynamic range required of accelerance measurements.

It is important that data are obtained at a sufficient number of appropriately planned locations. A 'grid' of points is generally used whereby the drive point response is measured at the mid-point of a sleeper bay and then, with the same response location, responses are obtained from four excitation points per sleeper bay for the first two and a half sleeper bays, at above-sleeper and mid-sleeper points for the next few sleeper bays. Beyond these, measurements are only required at mid-sleeper positions. The close spacing of the points initially (for the 'near field') is important to enable the reliable measurement of decay rates that are typically of the order of 10 dB/m at low frequency. For much lower decay rates, the more distant locations become important. For the longer distances responses are not required in every sleeper bay and the measurement locations are thinned out with distance accordingly. On periodically supported track it is essential that equivalent positions between supports be used because of the variation of response between supports near to, and above, the first 'pinned–pinned' frequency. This is not a constraint on continuously supported track but the general distribution of measurement points should be kept. In new proposals for the TSI's [3] a specific grid of points that was used by the Noemie project is being specified.

The decay rates for one-third octave frequency bands can, in principle, be estimated as the slope of a graph of band-averaged response in dB versus the distance z. This is the method that was first used [7,12]. The results were examined and a straight line fitted 'manually', requiring some experience to interpret the data.

The analysis of measured data assumes only one wave type in each of the vertical and lateral directions since only a single decay rate is extracted. However, in reality measurements show the effects of at least the near-field waves present in the simple track model as well as coupling between vertical and lateral waves, torsional waves and waves of cross-sectional modes. Cross-excitation may lead to a change in slope of a plot of response versus distance at the point at which the amplitude of an indirectly excited wave, if of lower decay rate, exceeds the amplitude of the wave of interest. In the estimation of the lateral decay rate, effects of beating between the lateral and torsional waves are encountered. The idealised, single exponential decay is also disrupted by the periodicity of the rail supports and the variation of response through a sleeper bay, particularly near the pinned–pinned resonances. These effects make it difficult to automate the line-fitting procedure and to remove the subjective element of such an analysis.

In practice, it is better to evaluate a decay rate based on a direct estimate of the summed response shown by Eq. (3) [13]. If A represents either the transfer accelerance or mobility then

$$\frac{1}{2\beta} = \int_0^\infty \frac{|A(z)|^2}{|A(0)|^2}\,\mathrm{d}z \approx \sum_{z_i=0}^{z_{\max}} \frac{|A(z_i)|^2}{|A(0)|^2}\,\Delta z_i, \tag{5}$$

where $z_{\max}$ is the maximum measurement distance and the sum is carried out for the response measurement locations. In line with the estimation of an integral by the midpoint rule where the intervals are not constant, for each location in the sum Δz_i should represent the distance between the mid-points to the locations either side. The influence of the interval taken for the measurement at $z_{\max}$ should be small but it would be chosen to be symmetrical about $z_{\max}$ and Δz_0 should be taken from $z = 0$. Thus

$$\varDelta \approx \frac{4.343|A(0)|^2}{\sum_{z_i=0}^{z_{\max}} |A(z_i)|^2\,\Delta z_i}. \tag{6}$$

Notice that an accurate measurement of $A(0)$ is important as it appears as a constant factor in the equation. In fact, of course, this is the location for which the response is most easily measured well.

This method of evaluation has been found to be robust for decay rates commonly encountered. By summing the response rather than fitting the slope to a graph on a dB scale, higher weighting is naturally given to the higher response values which are less likely to be contaminated by cross-coupling. The estimation may, however, be subject to error if the practical value of $z_{\max}$ truncates the integral in any one-third octave frequency band before a sufficient attenuation has taken place. From Eq. (6), a minimum value of decay rate that can be evaluated for a particular value of $z_{\max}$ can be estimated by supposing there to be no attenuation of A such that $A(z_i)$ is always equal to $A(0)$; thus

$$\varDelta_{\min} = \frac{4.343}{z_{\max}}. \tag{7}$$

The calculated decay rate should be compared with this value and if it is close to it, the estimation of decay rate should be deemed unsafe. In the first instance, measurements should be made to a sufficient distance to ensure that no significant error occurs. Of course, this is not always practicable for tracks with low decay rates and without knowing the decay rates a priori.

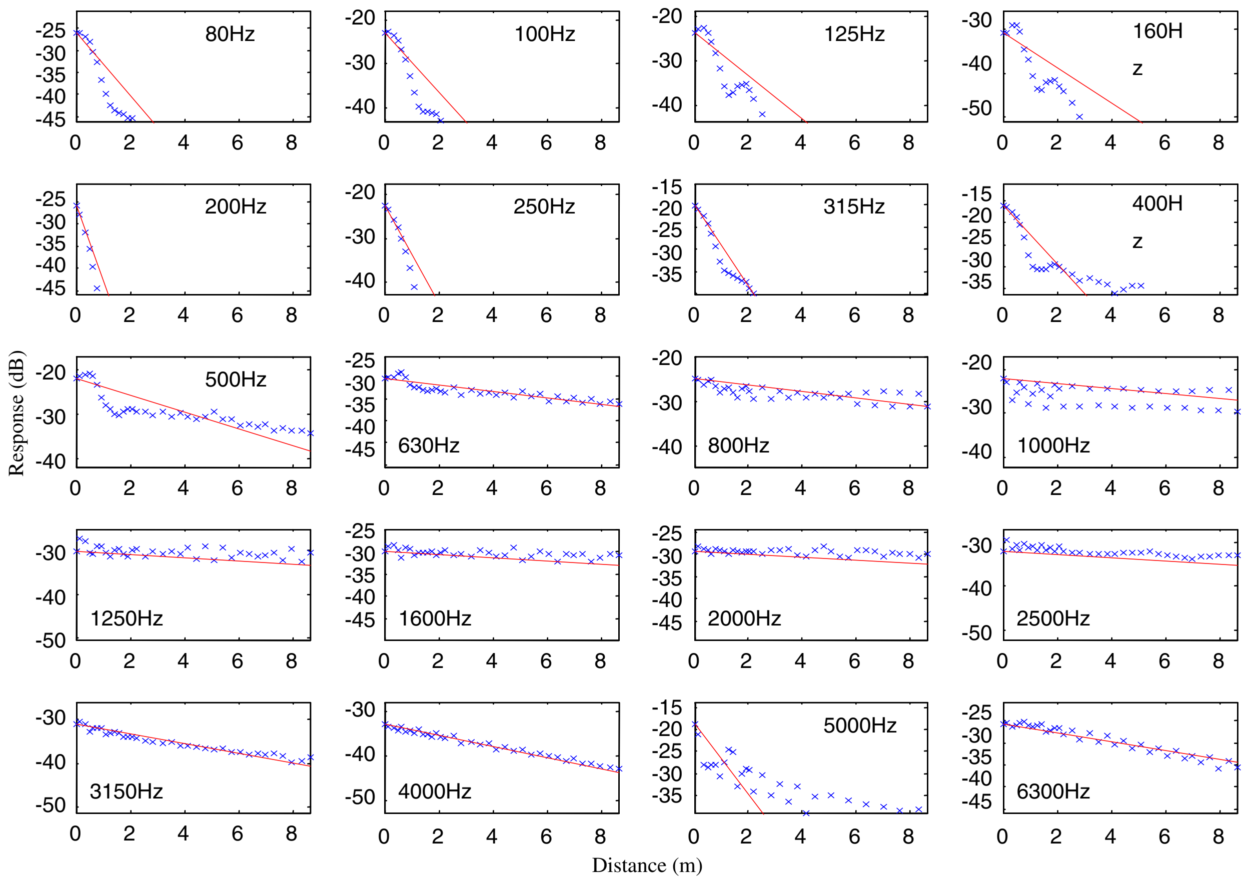

Fig. 1. Calculated vertical decay rates plotted in comparison with transfer response from 0 to 6 m for a ballasted track (× , measured response averaged in the band; ——, decay calculated using Eq. (6)). The range of response is the same on each graph.

Table 1
Parameters for the three tracks modelled using the simple beam track model (all with UIC 60 rails)

Track	Pad stiffness (loss factor)	Sleeper mass (spacing)	Ballast stiffness (loss factor)
Ballasted track, mono-bloc sleepers	200 MN/m (0.06)	125 kg (0.6 m)	150 MN/m (0.5)[a]
Slab track	2600 MN/m (0.25)	6[b] kg (0.65 m)	20[b] MN/m (0.2)
Ballasted track, bi-bloc sleepers	400 MN/m (0.2)	120 kg (0.6 m)	70 MN/m (0.7)

[a]For the result of Fig. 3 for this track, the sleeper is modelled as having modal behaviour and the ballast as having a frequency dependent stiffness. For the results of Fig. 2, the sleeper is modelled as a mass and the ballast as a constant stiffness (shown here).
[b]The baseplate mass is modelled as the 'sleeper' in the slab track and baseplate stiffness as that of the 'ballast'. The model is therefore constrained at the slab.

The decay rates can be checked by plotting them together with the measured response versus distance, for each one-third octave frequency band. Such a comparison for vertical response is shown in Fig. 1 for a ballasted track with UIC 60 rail, soft rail pads (200 MN/m) and with mono-bloc sleepers (see Table 1). Near-field effects can be seen throughout but especially in the low frequency bands up to 160 Hz. In the 500 Hz band, the relatively high response of the near-field wave and low decay rate of the propagating wave leads to a clearly higher estimate of the decay rate than that of the propagating wave alone. The effect of the pinned–pinned mode can be seen particularly in the 1 kHz band where midpoint responses are greater than those at above-sleeper positions. In the 5 kHz band the effects of the first vertical mode of the rail section, ('foot flapping' mode [6]) can be seen to increase the decay rate. This is due to the increased deformation it causes in the rail pad. In this band a lower amplitude wave is evident that has a lower decay rate.

For brevity, in the rest of the paper only decay rates of the vertical bending waves will be presented and discussed. However, the discussion applies equally to the lateral waves. The vertical vibration of the rail is more important than lateral for track with modern soft rail pads since it accounts for a greater proportion of the radiated noise.

4. Relationship between measured decay rate and the simple track model

In the next section, measured decay rates for three tracks are compared. First however, the relationship between the decay rates calculated by the wavenumber solution of a simple-beam track model and that calculated by the method described in Section 3, from the modelled response is studied for each of these tracks. They are a ballasted track with mono-bloc sleepers and a relatively soft rail pad (considered already above), a slab track with soft baseplates and a ballasted track with bi-bloc sleepers and a medium stiffness pad. The model parameters for each track are shown in Table 1.

The simple-beam model produces two complex wavenumbers each for vertical and lateral waves. One pertains to the wave that becomes propagating just above the resonance of the rail on the rail pad and the other to a near-field wave. The decaying part of the wavenumber relates directly to the decay rate as stated in Eq. (4). On the other hand, the decay rate calculated from the total response is that of a single equivalent wave whether the line fitting technique is used or the summation technique described here. Note that it has been the practice when using TWINS, sometimes, to impose the measured decay rate on the propagating wave predicted from the simple track model but also to leave the near-field wave in the calculation. This approximate method is useful if the predicted decay rate should be changed, for example for the effects of rail damping devices. It has been observed, however, that in normal circumstances the predicted decay rates may produce better TWINS noise predictions than do measured ones [4,8].

To illustrate the difference between the propagating wave decay rate, obtained from the simple-beam model, and the 'measured decay rate', the responses at the set of measurement locations have been calculated using the simple-beam model for each of the three tracks. The decay rates of the propagating wave only and those calculated from the responses are shown for each track in Fig. 2.

Fig. 2 shows that the decay rate calculated from the total response is close to that of the propagating wave especially for high frequencies. The greatest difference exists in each case for the frequency range just above the cut-on of propagation in the rail where the decay drops sharply. The difference is greatest for the slab track with the soft baseplate.

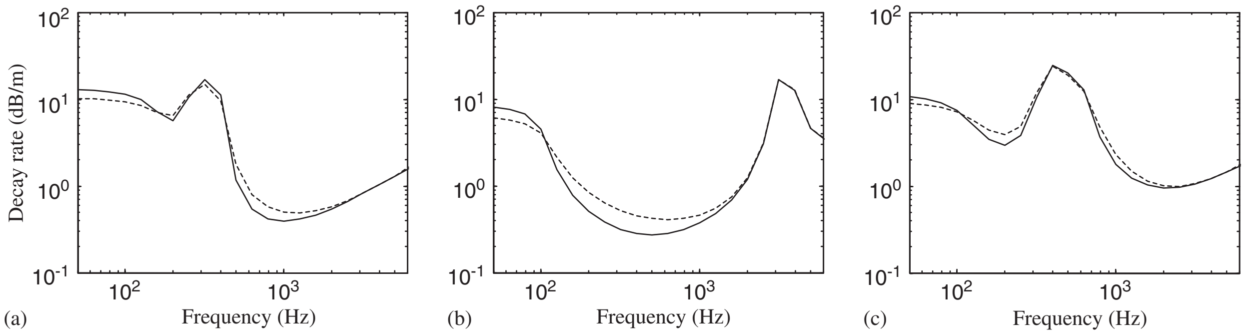

Fig. 2. Comparison of the propagating wave decay rate and the decay rate calculated from the response from the simple beam model: (a) for the ballasted track with mono-bloc sleepers; (b) for the slab track; and (c) for the ballasted track with bi-bloc sleepers (—, propagating wave; - - -, from response) (scales as for Fig. 3).

5. Measured decay rates

The measured decay rates indicated in Fig. 1 are for the ballasted track with mono-bloc sleepers and are plotted as a spectrum in Fig. 3 in comparison with the decay rate of the propagating wave of the simple track model. At low frequency the decay rates are high. Just above the resonance frequency of the rail on the pad (about 300 Hz), the rail becomes decoupled from the sleepers and, as the propagating wave cuts on, the decay rates become low. A strong peak can be seen around 5 kHz due to the foot-flapping mode of the rail. In this set of results no significant peak or dip is seen around the pinned–pinned frequency at 1 kHz even though the effect is clearly indicated in the response data (Fig. 1). For this set of measurements, the maximum measurement distance was only 14 m and the results are close to the minimum that this would suggest is calculable (Eq. (7)). However, this does not seem to have affected the calculated values significantly, as can be verified from Fig. 1.

Note that the decay rate, shown in Fig. 3, calculated from the propagating wavenumber of the simple track model also has the effect of the sleeper modes and frequency-dependent ballast stiffness taken into account (unlike the result presented in Fig. 2(a)). Given the known discrepancy between the two definitions of decay rate illustrated in Fig. 2(a), and that the effect of the foot-flapping mode is not present in the simple track model, the comparison of decay rates (Fig. 3) shows that an accurate model of the track has been achieved. Even the small undulations in the spectrum due to the sleeper and ballast layer modes (in the range 500 Hz–1 kHz) are reproduced, at least qualitatively.

Fig. 4 presents the decay rates measured on the slab track. Here, because of the soft supports, the propagating wave cuts on at about 120 Hz and the decay rate becomes very low. This drop in decay rate is modelled accurately by the use of the stated design stiffness of the soft lower pad. Even though there is a significant discrepancy between the two definitions of decay rate to be taken into account (Fig. 2(b)), there is a clear difference in the frequency range 200 Hz–2 kHz for the vertical decay rate. Large peaks in the measured decay rate are seen in the 800 Hz and 3.15 kHz bands. In the model the strong peak at 3.15 kHz is due to the baseplate mass acting as a tuned absorber; the resonance is that of the baseplate mass on the stiffness of the upper pad. The decay rate is predicted as being much lower than measured between 200 Hz and 1.6 kHz. A plot similar to Fig. 1 (not presented) shows nothing to suggest that the response measurements

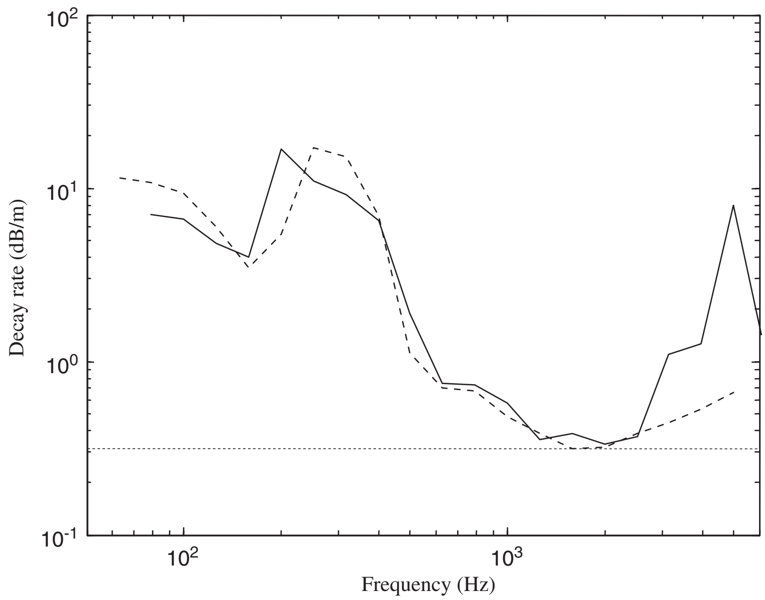

Fig. 3. Decay rates for the ballasted, mono-bloc sleeper track calculated by Eq. (5) plotted in comparison with the decay rate of the propagating wave predicted using the simple track model; —, measured decay rate; - - -, predicted decay rate; · · · · · ·, minimum measurable decay rate.

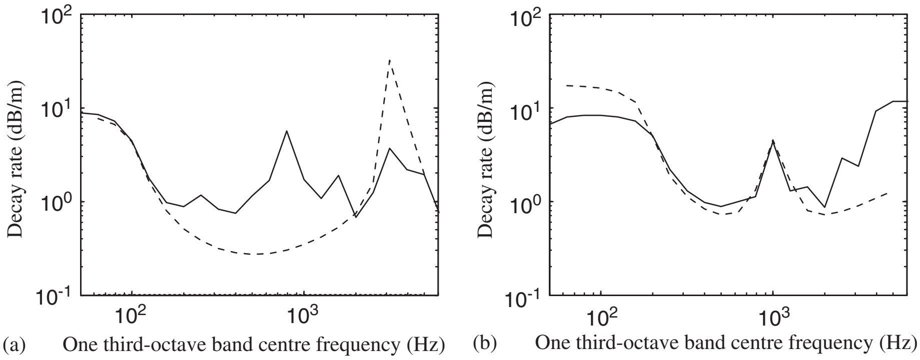

Fig. 4. Measured decay rates of the slab track plotted in comparison with the decay rate of the propagating wave predicted using the simple track model: (a) vertical decay rates; (b) lateral decay rates; —, measured; - - -, predicted; · · · · · ·, minimum measurable decay rate.

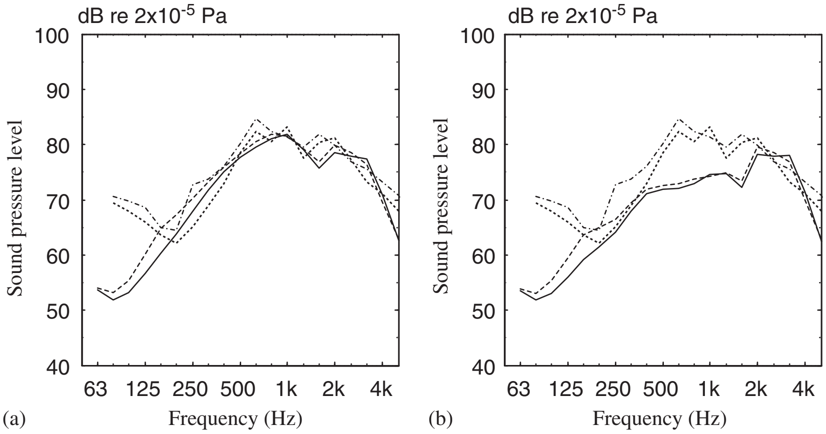

Fig. 5. Measured and predicted sound pressure level at 7.5 m for two different wheel types (A and B) of a train running on the slab track at 120 km/h: (a) predictions using the calculated decay rates; (b) predictions using the measured decay rates; —, predicted for wheels A, 89.8 dB (A) in (a) and 86.0 dB (A) in (b); - - -, predicted for wheels B, 90.3 dB (B) in (a) and 86.4 dB (B) in (b); - · - ·, measured for wheels A, 89.8 dB (A); · · · · · ·, measured for wheels B, 90.5 dB (B).

or the decay rate calculation are untrustworthy. The peak in the measurement in the 800 Hz band suggests the upper pad stiffness could be modelled as much lower than the value assumed but it is inconceivable that the stiffness of a thin plastic pad should be around the 100 MN/m required to locate the peak in the 800 Hz band rather than the realistic value used. In any case, for this example, the lateral decay rates are also plotted in Fig. 4 to show that the corresponding effect there is modelled comparatively well with the very stiff upper pad.

For the slab track, Fig. 5 presents measured rolling noise at 7.5 m along with TWINS predictions based on measured wheel and rail roughnesses and the (laboratory-measured) track parameters given in Table 1. It can be seen that use of the predicted decay rates produces an accurate noise prediction whereas the measured decay rates produce a substantial under-prediction. It may be concluded that the decay rates of the track under the train loading do not operate during measurements on the unloaded track. It has already been shown with more detailed track models that the effects of the train loading can *increase* the effective decay rate [14] but this is clearly not the effect operating here.

The measured and predicted decay rates of the third track are presented in Fig. 6. In this case, only points at mid-sleeper were used in the measurement beyond the third sleeper bay. Here it can be seen that, besides the lack of the foot-flapping mode effect, the model agrees with the measurements except at a significant peak in

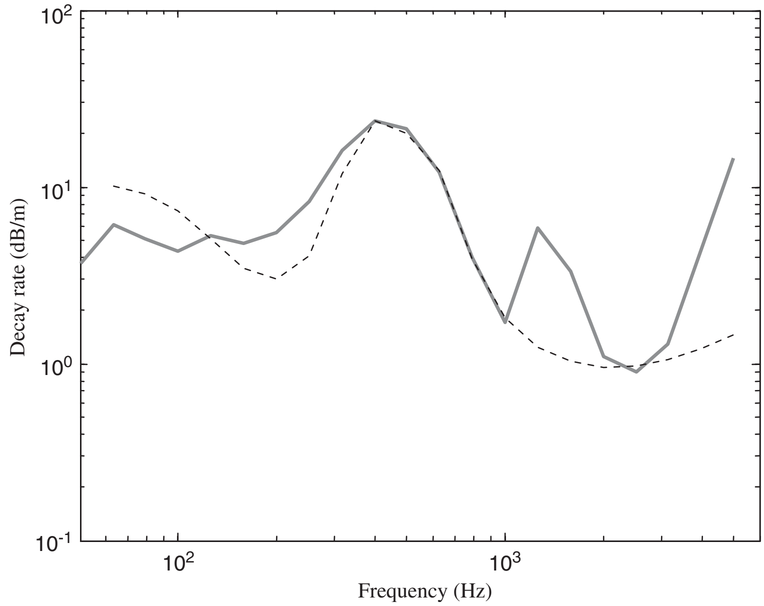

Fig. 6. Measured vertical decay rates and those calculated using the simple track model for the bi-bloc sleeper track; ▬▬, measured; - - - -, predicted.

the measured decay rates in the 1.25 and 1.6 kHz bands. To investigate the origins of this, a more detailed track model is used.

6. Decay rates calculated using a periodically supported track model

The track model, 'Cobra', is based on composite beam models for the vertical and lateral dynamics of an infinite rail supported at a finite, but large number of sleepers [15,16]. The model therefore includes the effect of cross-sectional deformation at high frequency and the effects of the pinned–pinned resonances in the rail. In this model the decay rates are calculated from the responses. They therefore correspond to the measurement method except that a very large number of response points can be used. Additionally, the calculation can be carried out for a number of contact positions within a sleeper span so that the vibration response and resulting noise radiation can be averaged to represent that of a moving train.

Fig. 7 presents an example of the decay rates for the bi-bloc-sleeper track, calculated with Cobra with regularly spaced sleepers. Four calculated curves are shown. The first is calculated as the mean for five positions of the wheel-contact point in a sleeper bay; 500 response points along 60 m of rail are used. These are all at the centre of the rail-head so that the lateral response is uncoupled from the vertical response. The agreement with the measured curve is good up to about 1 kHz. With this model, a peak appears in the 1.25 kHz band that is an effect of the behaviour at a frequency just above that of the first pinned–pinned mode of the rail at about 1 kHz [14]. However, the predicted peak is not as high as the measured peak. At frequencies higher than this, the calculation produces lower decay rates than the measurement.

Another calculation indicates the role of coupling between the vertical and lateral motion of the rail. For this calculation the contact and response points are all offset by 15 mm from the rail-head centre-line. This indicates (Fig. 7) a higher decay rate above 2 kHz as energy transfers from the vertical bending of the rail into other wave types (lateral, torsional, web-bending) and a good agreement with the measurement in this frequency range is obtained. Since such coupling will be present in practice the higher decay rate in this frequency range is appropriate to use in noise predictions.

In order to investigate the peak in the 1.25 kHz band, a further calculated result is shown in Fig. 7 in which the wheel-contact position is at the mid-span and only mid-span response points are used. The 15 mm offset is kept. In this case the peak just above the pinned–pinned resonance has a similar height to the measured one.

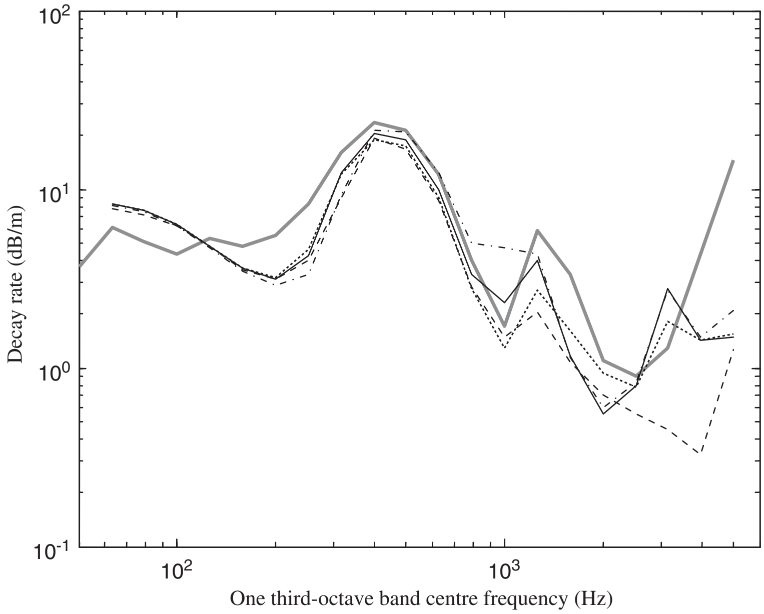

Fig. 7. Measured vertical decay rate and those calculated using the Cobra track model for the bi-bloc sleeper track; ▬▬, measured; - - - -, predicted with 5 wheel-contact locations in the sleeper bay and many response points but no lateral offset; · · · · · ·, predicted with a 15 mm lateral offset; - · - ·, predicted with the lateral offset and only response points at mid-span; —, predicted with the lateral offset and response points at mid-span and above sleeper.

This indicates that the peak is a function of the use of a grid of measurement locations with over-emphasis on the mid-point response.

Looking back at the measurement on the mono-bloc sleepered track, Fig. 3, it is clear that there is no evidence of a peak in the 1.25 kHz band despite there being clear evidence of strong pinned–pinned behaviour in the responses (Fig. 1). To investigate the influence of this set of measurement points, an additional calculation for the bi-bloc track with the single mid-span excitation point has been carried out that uses response points at mid-span and above sleepers throughout the range measured. This is also plotted in Fig. 7. This leads to a reduced estimate of decay rate in the 1 kHz band but not to a reduction in the height of the peak at 1.25 kHz.

None of this explains the absence of a peak in the results of Fig. 3 although predictions show that the softer rail pad reduces the effect (not presented).

It is notable that the very strong effect of the foot-flapping mode in raising the decay rate at 5 kHz is not reproduced to the same extent by the Cobra model although the point receptance is reproduced correctly in this respect [15]. This may be a shortcoming of the model.

7. Conclusions

A direct and automated method for calculating the decay rates from measurement data has been proposed that can be used to calculate an equivalent vertical and lateral wave decay rate for the track. The measured equivalent single decay rate (for vibration in each direction) is a suitable measure to characterise the acoustic performance of a track and is close to the predicted decay rates from track models. However, it is not strictly the same as the decay rate of the propagating wave in the simple track model that it has been used to replace in some noise predictions.

Although the track models have been shown to predict decay rates well in most cases, it has been demonstrated with the slab-track example that the measured decay rate may not, as in this case, correspond well to the prediction. It is the predicted, rather than the measured, decay rate that produces a good noise prediction in this case.

The example of the bi-bloc sleepered track shows a peak in the measured decay rate at 1.25 kHz that is only reproduced by a model that includes the effects of discrete supports. It is shown that the height of the peak that is measured is sensitive to the set of measurement locations and that the real effect is somewhat smaller than measured.

Acknowledgements

The authors are grateful for permission to use data measured by the Agence d'Essai Ferroviaire of the SNCF for the Noemie project of the Association Européenne pour l'Interoperbilité Ferroviaire (AEIF).

References

[1] Directive 2001/16/EC of the European parliament and of the Council of 19 March 2001 on the interoperability of the trans-European conventional rail system, *Official Journal of the European Communities*, 2 April 2001.
[2] Commission decision of 30th May 2002 concerning the technical specification for interoperability relating to the rolling stock subsystem of the trans-European high-speed rail system referred to in Article 6(1) of Directive 96/48/EC, reference 2002/735/EC, *Official Journal of the European Communities*, 12 September 2002.
[3] P. Fodiman, Improvement of the noise technical specifications for interoperability: the input of the Noemie project, *Proceedings of the 8th International Workshop on Railway Noise*, Buxton, England, 2004. (Should be updated to be the JSV version of this paper in the same issue.)
[4] D.J. Thompson, P. Fodiman, H. Mahé, Experimental validation of the Twins prediction program for rolling noise, part 2: results, *Journal of Sound and Vibration* 193 (1996) 137–147.
[5] D.J. Thompson, C.J.C. Jones, A review of the modelling of wheel/rail noise generation, *Journal of Sound and Vibration* 231 (2000) 519–536.
[6] D.J. Thompson, Experimental analysis of wave propagation in railway tracks, *Journal of Sound and Vibration* 203 (1997) 867–888.
[7] D.J. Thompson, B. Hemsworth, N. Vincent, Experimental validation of the Twins prediction program for rolling noise, part 1: description of the model and method, *Journal of Sound and Vibration* 193 (1996) 123–135.
[8] C.J.C. Jones, D.J. Thompson, Extended validation of a theoretical model for railway rolling noise using novel wheel and track designs, *Journal of Sound and Vibration* 267 (2003) 509–522.
[9] D.J. Thompson, Wheel–rail noise generation, part IV: contact zone and results, *Journal of Sound and Vibration* 161 (1993) 447–466.
[10] D.J. Thompson, N. Vincent, Track dynamic behaviour at high frequencies. Part 1: theoretical models and laboratory measurements, *Vehicle System Dynamics Supplement* 24 (1995) 86–99.
[11] D.J. Thompson, C.J.C. Jones, N. Turner, Investigation into the validity of two-dimensional models for sound radiation from waves in rails, *Journal of the Acoustical Society of America* 113 (2003) 1965–1974.
[12] N. Vincent, D.J. Thompson, Track dynamic behaviour at high frequencies. Part 2: experimental results and comparisons with theory, *Vehicle System Dynamics Supplement* 24 (1995) 100–114.
[13] G. de France, Railway Track: Effect of Rail Support Stiffness on Vibration and Noise, MSc Dissertation, Institute of Sound and Vibration, University of Southampton, 1998.
[14] D.J. Thompson, C.J.C. Jones, T.X. Wu, G. de France, The influence of the non-linear stiffness behaviour of rail pads on the track component of rolling noise, *Proceedings of the Institution of Mechanical Engineers Part F* 213 (1999) 233–241.
[15] C.J.C. Jones, D.J. Thompson, T.X. Wu, An advanced track model for use in the prediction of wheel–rail rolling noise, *Proceedings of Euronoise 2003*, *Fifth European Conference on Noise Control*, 2003, Paper 044 on CD-ROM.
[16] T.X. Wu, Development and Application of Theoretical Models for High Frequency Vibration of Railway Track, PhD Thesis, University of Southampton, 2000.